Sensors and Materials, Vol. 34, No. 8 (2022) 3339–3358
MYU Tokyo

S & M 3044

"First Kilometer" Scheduling Task of Multiple Unmanned Aerial Vehicles Based on Multisource Heterogeneous Sensors

Xiaohua Yang,[1] Miaohan Zhang,[2*] Nan Pan,[2] Shiyun Chen,[2] and Yuhang Han[2]

[1]Measurement Center, Yunnan Power Grid Co., Ltd., Kunming 650051, China
[2]Faculty of Civil Aviation and Aeronautics, Kunming University of Science and Technology, Kunming 650500, China

(Received April 7, 2022; accepted August 2, 2022)

Keywords: UAVs, path planning, logistics scheduling, whale algorithm, multisource heterogeneous sensors

To solve the problem of "first-kilometer" distribution difficulties in rural areas, we propose a transportation method using unmanned aerial vehicles (UAVs) for delivery. The mountainous environment of Fengshan County in Guizhou is first simulated as the UAV delivery environment. A differential evolution strategy based on the improved whale optimization algorithm (DEIWOA) combined with multisource heterogeneous sensors is then proposed to solve the UAV obstacle avoidance path. After the UAV's delivery path is planned using the DEIWOA algorithm, the multisource heterogeneous sensor is used to perform obstacle avoidance among multiple UAVs and path correction of UAVs in actual situations. Afterwards, to minimize the delivery cost of UAVs, a multi-UAV cargo delivery model is built with the optimization goal of minimizing the transportation cost and time window violation cost. This UAV scheduling model is solved using the proposed DEIWOA algorithm. Finally, simulations are performed to compare the proposed method with the cutting-edge algorithms. The obtained results show that the proposed DEIWOA algorithm can provide a better plan of the UAV path and reduce the cost of logistics scheduling. It can also provide support for UAV logistics and distribution in mountainous areas in actual situations.

1. Introduction

In recent years, in the context of new rural development, agricultural logistics has become a vital guarantee to promote the development of a rural economy. Because of the complex terrain environment in some poor mountainous areas, ground transportation faces great difficulties, and the traditional logistics and distribution methods cannot meet the dual demands of timeliness and freshness in the transport of agricultural products.(1) The complex rural "first-kilometer" distribution has been widely studied by researchers and industries, since an efficient distribution is crucial for improving the economic development in poor mountainous areas. UAVs have high flexibility, fast speed, minor transportation restrictions, and high economic efficiency.(2) Therefore, in this paper, we propose a distribution model that uses UAVs to transport fresh agricultural products from the

*Corresponding author: e-mail: 957280927@qq.com
https://doi.org/10.18494/SAM3935

ISSN 0914-4935
https://myukk.org/

rural site (shipping point) to the ground cold vehicle (receiving point) outside the mountainous area.

Agricultural products such as mushrooms and *matsutake* mushrooms have the characteristics of high value, lightweight, and short storage time. The attributes of the freshness of the agricultural products should be considered when designing the UAV delivery solution. The value of the agricultural products can be retained to the greatest extent only when the UAV delivers the agricultural products as fast as possible within the service time limit of the receiving point. Therefore, the UAV "first-kilometer" delivery problem is similar to the vehicle path planning problem, which can be understood as a multi-UAV path planning and scheduling problem with time windows. To solve this problem, the UAV path planning and UAV task order assignment in the 3D environment should be considered.

The UAV delivery problem is an expansion of the vehicle path problem in 3D space. The current studies on UAV delivery mainly focus on the transport to the client side and the UAV route plan. The established optimization objectives mainly include the minimization of the delivery cost and the maximization of customer satisfaction.[3,4] Zhang *et al.*[5] conducted an in-depth study of the logistics UAV delivery problem, while considering several factors such as the performance of the UAV and the nature of the mission. They then developed a multi-objective function to minimize the range, navigation altitude, and crash hazard of the UAV. Qiqian *et al.*[6] explored the UAV logistics model to reduce the cost of the UAV logistics system and expand the distribution area through the study of public transport networks. Since the swarm intelligence algorithm can quickly solve UAV paths while mostly avoiding falling into a local optimum, the use of the swarm intelligence algorithm to solve UAV paths has become crucial.[7,8] For example, in the study of multi-UAV trajectory planning, optimization algorithms such as the genetic algorithm and ant colony algorithm were widely used to solve the trajectory planning problem of UAVs.[9,10]

Most of the current logistics scheduling optimization methods focus on the shortest path (the traveling salesman problem, TSP) planning or the maximization of the economic efficiency of allocation while considering time window constraints. Li *et al.*[11] proposed to solve the vehicle routing problem (VRP) with a soft time window by introducing the interindividual merit search strategy of fireflies into the ant colony algorithm to improve the robustness and feasibility of the algorithm, thereby solving the logistics scheduling distribution. Zheng[12] proposed the machine learning algorithm using the Gaussian process to speed up the convergence of the algorithm. In deterministic time window algorithm planning, Fan *et al.*[13] developed an adaptive perturbation mechanism with a variable neighborhood descent search as the main body. They solved the soft time window vehicle path problem with simultaneous set dispensing by combining the domain search strategy with the particle swarm algorithm, which improved the ability to explore the solution space and the algorithm's global search capacity. In addition, Lu *et al.*[14] combined the simulated annealing algorithm with the A* (A-star) algorithm to solve the path planning logistics scheduling problem for different purposes. Tiwari *et al.*[15] proposed a study of UAV trajectory planning in dynamic environments using multiverse algorithms.

With the rapid development of UAV logistics scheduling, many researchers have conducted in-depth studies on the UAV logistics delivery problem. However, in the construction of the delivery model, the mission planning of the UAV in a two-dimensional environment is mainly considered

while ignoring the different limitations in a three-dimensional environment. Therefore, in this paper, the 3D path planning of UAVs is combined with mission path planning to construct a multi-UAV scheduling model in a multidimensional constrained environment. Moreover, the concept of multisource heterogeneous sensors is introduced to help the UAVs perform timely obstacle avoidance and path correction during actual missions. Finally, an improved whale optimization algorithm is designed for the UAV's 3D obstacle avoidance path determination and optimal path task assignment.

2. Task Description

To solve the problem of difficult rural delivery, we have established a delivery model for multiple UAVs, whose task description is shown below. It is first assumed that the rural shipping point receives the order for goods. Then the goods are loaded onto the UAV at the rural shipping point, and delivery is performed following the planned path. The UAV performs real-time obstacle avoidance through the use of multisource heterogeneous sensors during the delivery task. Finally, the UAV returns to the shipping point after delivering the goods to the receiving point, i.e., the ground-based cold delivery vehicle, with multiple time windows. The delivery path diagram of the UAV is shown in Fig. 1. The technical framework of this study is shown in Fig. 2.

In Fig. 1, the red stars (numbers 1, 2, and 3) are rural delivery points. Afterwards, the UAVs further deliver the goods to the ground-based cold delivery vehicles, i.e., the receiving points (numbers 4, 5, 6, 7, and 8).

The UAV first loads cargo at the rural shipping point. Then, under the performance constraints of the maximum load, the longest running time, elevation angle, and deflection angle, the path planning model of the UAV from the rural shipping point to the cold transport vehicle (receiving point) is established, and the three-dimensional virtual path of the UAV is obtained through the algorithm designed in this paper. On this basis, to ensure that the UAV is not affected by dynamic obstacles in the distribution process, multisource heterogeneous sensors are added to the UAV. These sensors perform the dynamic real-time obstacle avoidance of the UAV. When the sensor detects obstacles in the front, it will change the current UAV path. The sensor will plan the UAV

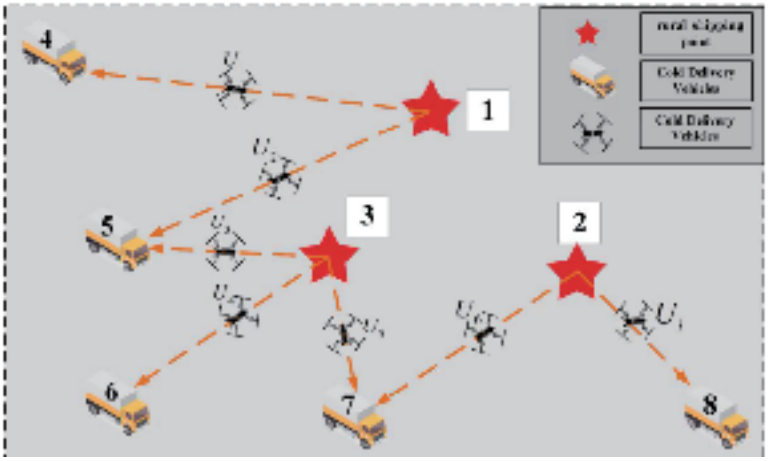

Fig. 1. (Color online) UAV delivery path diagram.

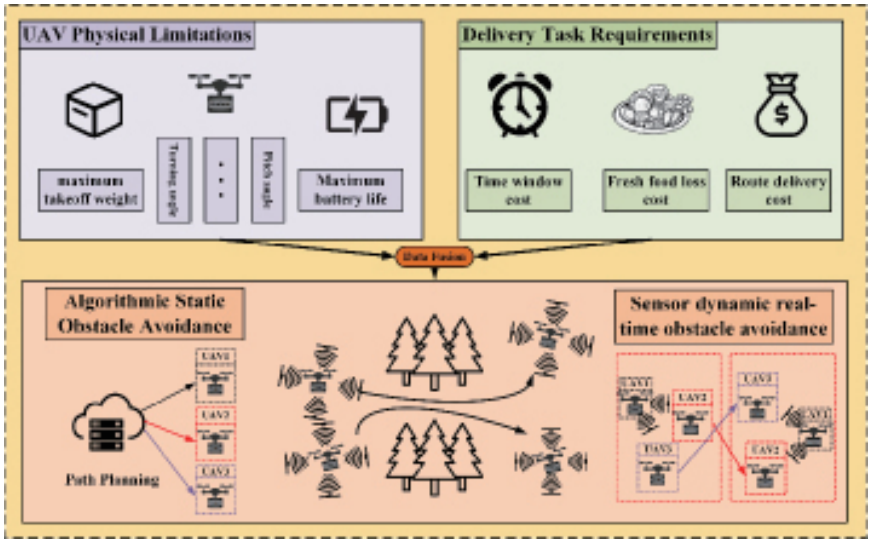

Fig. 2. (Color online) Scheduling task architecture.

to fly back to the original path when the obstacle in front has been avoided. Finally, the cost of the UAV distribution path, the cost of fresh agricultural products, and the service time window of each cold delivery vehicle (receiving point) are considered as crucial factors for the development of the multi-UAV logistics scheduling task planning model. Finally, the algorithm is designed to solve the model, and the optimal UAV order distribution scheme (vehicle dispatch model) is obtained.

2.1 Model assumptions

The delivery tasks of UAVs have the requirements of long-distance transportation and high timeliness. Therefore, their dispatching process is different from that of general ground vehicles. Consequently, the 3D path planning of UAVs and the logistics scheduling and distribution scheme should be simultaneously considered in the model construction. In this study, the following assumptions are made.

(1) The locations of the rural shipping point and the ground cold delivery vehicle receiving point are known. The number of orders received at each rural shipping point is known, and the number of UAVs is definitively fixed.
(2) The unloading service time for UAVs delivering products to cold delivery vehicles is fixed, allowing multiple UAVs to simultaneously unload.
(3) Each ground cold delivery vehicle has a specific time window that the UAV needs to meet to minimize the cost of the resulting time window violation penalties during the delivery process.
(4) No complex movements of UAVs are involved in the delivery process.
(5) The UAVs should return to the rural shipping point after completing the delivery task.

2.2 Symbol definition

The variables and symbols used in this paper are shown in Table 1.

Table 1
Descriptions of mathematical model symbols.

Symbols	Meaning
i	The i-th rural (shipping point) $i = 1, 2, ..., I$.
j	The j-th ground cold delivery vehicle (receiving point).
U_i^k	The k-th UAV at shipping point i, $k = 1, 2, ..., K$.
$x_{i,j}^k$	0–1 variable indicating whether the k-th UAV departs from shipping point i to reach receiving point j.
$[T_{start}^i, T_{finish}^i]$	Working time window for the i-th rural shipping point.
$[T_{start}^j, T_{finish}^j]$	Working time window for the j-th cold delivery vehicle (receiving point).
$t_{i,j}^k$	Time required for the k-th UAV at the i-th shipping point to travel to the j-th receiving point.
v_t^k	Speed of the k-th UAV
$t_{i,start}^k$	Time of departure of the k-th UAV from shipping point i.
$t_{i,finish}^k$	Time of return to shipping point i for the k-th UAV
$t_{j,start}^k$	Time of arrival of the k-th UAV at receiving point j.
$t_{j,finish}^k$	Time when the k-th UAV leaves receiving point j.
Dis_{ij}	Euclidean distance between shipping point i and receiving point j.
R_j	Order requirements for the j-th receiving point.
p_1^j	Penalty factor for early arrival of the UAV at receiving point j.
p_2^j	Penalty factor for delayed arrival of the UAV at receiving point j.
$d_{i,j}^k$	Delivery distance of the k-th UAV.
t_{max}	Maximum endurance of the UAV.
w_{max}	UAV Maximum payload.
α_m^k	Coefficient of freshness per unit mass of raw product m with time t.
m_t^k	Weight of the k-th UAV at moment t.
βmax	UAV turning angle.
λ_{max}	UAV pitch angle.
d_{max}	Maximum range of the UAV.
H_{max}	Maximum flight height of the UAV.
H_{min}	Minimum flight altitude for the UAV.
M	Maximum load that the UAV can handle.
p_u	Price per unit quality of fresh produce.
a	UAV delivery cost.
b	UAV cost per kilometer of delivery path.
D_{max}	Maximum flight distance of the UAV.
R_i	Maximum number of shipments that can be provided by shipping point i.
d_{safe}^A	Danger-warning distance for sensor-aware radar.
$\left(x_{i'}^*, y_{i'}^*, z_{i'}^*\right)$	Coordinates of the i-th obstacle.

2.3 Model construction

2.3.1 Decision variable

In this study, $x_{i,j}^{k}$ denotes that the k-th UAV performs the transportation mission from shipping point i to receiving point j. If this delivery exists, $x_{i,j}^{k}$ takes the value of 1. If not, it takes the value of 0. If the order of the j-th receiving point is served by the k-th UAV, then $y_{j}^{k} = 1$. If it does not exist, $y_{j}^{k} = 0$.

2.3.2 Objective function

The optimization objectives of this study are to minimize the logistics delivery cost (Z_1), the value loss of fresh commodities (Z_2), and the penalty costs incurred by the violation of the time window (Z_3 and Z_4). The proposed model of UAV delivery under the considered time window is summarized as follows.

The logistics cost incurred in UAV delivery is composed of the number of UAVs and the path length of the UAVs.

$$d_{i,j} = \sum_{i=1}^{N-1} \sqrt{(x_{i+1} - x_i)^2 + (y_{i+1} - y_i)^2 + (z_{i+1} - z_i)^2} \tag{1}$$

$$\min Z_1 = \min(aK + b\sum_{i=1}^{I}\sum_{j=1}^{J}\sum_{k=1}^{K} d_{i,j} x_{i,j}^{k}) \tag{2}$$

The cost of time loss of fresh commodities arising during UAV transport is given below.

$$\min Z_2 = \sum_{j=1, j\in J}^{J} \sum_{k\in K} \sum_{i\in I} \sum_{m\in M} x_{i,j}^{k} R_j p_u [1 - \alpha_m^k (t_{j,start}^{k} - t_{i,start}^{k})] \tag{3}$$

The total cost of waiting time incurred by the UAV throughout the soft time window violation is computed as follows.

$$\min Z_3 = \sum_{k=1}^{K}\sum_{i=1}^{I}\sum_{j=1}^{J} x_{i,j}^{k} p_1^j [\max(T_{start}^{j} - t_{i,j}^{k}, 0)] + \sum_{k=1}^{K}\sum_{i=1}^{I}\sum_{j=1}^{J} x_{i,j}^{k} p_1^j [\max(T_{finish}^{i} - t_{j,i}^{k}, 0)] \tag{4}$$

The total cost in excess of time incurred by the UAVs throughout the violation of the soft time window is calculated.

$$\min Z_4 = \sum_{k=1}^{K}\sum_{i=1}^{I}\sum_{j=1}^{J} x_{i,j}^{k} p_2^j [\max(t_{i,j}^{k} - T_{start}^{j}, 0)] + \sum_{k=1}^{K}\sum_{i=1}^{I}\sum_{j=1}^{J} x_{i,j}^{k} p_2^j [\max(t_{j,i}^{k} - T_{finish}^{i}, 0)] \tag{5}$$

The objective function of our established model is to minimize the cost of drone scheduling, minimize the cost of raw loss, and minimize the penalty cost incurred by the drone for violating the time window. The established objective function is shown as Eq. (6).

$$y = \min(Z_1 + Z_2 + Z_3 + Z_4) \tag{6}$$

$$\sum_{i\in I}\sum_{j\in J}\sum_{k\in K} x_{i,j}^{k} d_{i,j} \le D_{max} \tag{7}$$

$$H_{min} < h^{k} < H_{max} \tag{8}$$

$$\sum_{i=1}^{I}\sum_{j=1}^{J} x_{i,j}^{k} \le 2, \quad \forall k \in K \tag{9}$$

$$\sum_{i=1}^{I}\sum_{j=1}^{J} x_{i,j}^{k} - \sum_{j=1}^{J}\sum_{i=1}^{I} x_{j,i}^{k} = 0, \quad \forall k \in K \tag{10}$$

$$\sum_{i\in I}\sum_{j\in J} w_{i,j}^{k} \le w_{max}, \quad \forall k \in K \tag{11}$$

$$0 < \arccos\left[\frac{(x_{i+1}^{A} - x_{i}^{A})(x_{i}^{A} - x_{i-1}^{A}) + (y_{i+1}^{A} - y_{i}^{A})(y_{i}^{A} - y_{i-1}^{A})}{\sqrt{(x_{i+1}^{A} - x_{i}^{A})^2 + (x_{i}^{A} - x_{i-1}^{A})^2}\sqrt{(y_{i+1}^{A} - y_{i}^{A})^2 + (y_{i}^{A} - y_{i-1}^{A})^2}}\right] \le \beta_{max}, \quad z^{m} = z^{m+1} \tag{12}$$

$$0 < \arctan\left[\frac{\left|z_{i}^{A} - z_{i-1}^{A}\right|}{\sqrt{(x_{i}^{A} - x_{i-1}^{A})^2 + (y_{i}^{A} - y_{i-1}^{A})^2}}\right] \le \lambda_{max}, \quad (z^{m} \ne z^{m+1}) \tag{13}$$

$$\sum_{i\in I}\sum_{j\in J}\sum_{k\in K} t_{i,j}^{k} + \sum_{i\in I}\sum_{j\in J}\sum_{k\in K} t_{j,i}^{k} \le t_{max} \tag{14}$$

$$0 \le \sum_{n\in N}\sum_{k\in K} v_{n}^{k} \le v_{max} \tag{15}$$

$$t_{min} \le \sum_{n\in N}\sum_{k\in K} t_{n}^{k} \le t_{max} \tag{16}$$

$$\sum_{k=1}^{m}\sum_{j=1}^{J}\sum_{i=1}^{I} x_{i,j}^{k} \le K, \quad \forall k \in K \tag{17}$$

$$\sum_{j=1}^{J} R_J \le \sum_{i=1}^{I} R_I, \forall i \in I, \quad j \in J \tag{18}$$

$$d_{ii'}^{A}=\sqrt{\left(x_i^A-x_{i'}^*\right)^2+\left(y_i^A-y_{i'}^*\right)^2+\left(z_i^A-z_{i'}^*\right)^2}$$
$$d_{ii'}^{A}\geq d_{safe}^{A} \tag{19}$$

Equation (7) indicates that the flight distance of the UAV is less than its maximum flight distance. Equation (8) indicates that the flight height of the UAV is limited. Equation (9) represents the UAV delivery to a maximum of two receiving points in one mission. Equation (10) indicates that the UAV should return to the rural delivery point after completing the delivery task. Equation (11) indicates that the maximum load limit should be satisfied during the delivery by the UAV. Equation (12) indicates that the UAV should satisfy the turning angle constraint. Equation (13) indicates that the UAV should satisfy the pitch angle constraint. Equation (14) indicates that the UAV should satisfy the actual time constraint throughout the delivery time. Equation (15) indicates that the flight speed of the UAV at each stage should meet its performance speed constraint. Equation (16) indicates that the total flight time of the UAV should satisfy its performance. Equation (17) indicates that the UAVs required for delivery is within the limit of the total number of UAVs allowed. Equation (18) shows that the quantity of goods provided by rural shipping points can fully meet the demand of order quantity. Equation (19) indicates that the distance between the UAV and the obstacle is greater than the hazard sensing distance of the sensor radar.

3. Differential Evolution Strategy Based on Improved Whale Optimization Algorithm (DEIWOA)

3.1 Traditional whale optimization algorithm

The WOA is a novel population intelligence optimization algorithm inspired by the bubble predation strategy. It has three main stages: contraction surround process, random search prey process, and bubble net attack process. In the traditional whale algorithm, the number of whales and the search space dimension are defined as *Nop* and *D*, respectively. In addition, the location is defined as $W_i=(W_i^1,W_i^2,...,W_i^D)$; $i=1,2,...,Nop$, and $Fitness_i$ represents each whale's corresponding fitness function value, where the position of the prey is the optimal position of the whale. Compared with other swarm intelligence optimization algorithms, the whale optimization algorithm is characterized by a high search ability, few required parameters, and easy implementation. Therefore, this algorithm is widely used in the field of logistics scheduling.

3.1.1 Contraction surround process

In the global search, the best search position of the whale population is usually the known optimal solution (prey) or the position of the whale nearest the target. Moreover, the rest of the whale individuals approach the optimal solution (i.e., the optimal whale position) by gradually encircling the prey, thus performing the global search. The mathematical model of this update is given by

$$D = \left| C \cdot W^*(t) - W(t) \right|, \tag{20}$$

$$W(t+1) = W^*(t) - A \cdot D, \tag{21}$$

where D is the distance between an individual whale and the optimal whale in the population, t is the current number of iterations, $W^*(t)$ is the optimal position of the whale individual, $W(t)$ is the position of the whale individual in the current iteration, $W(t + 1)$ is the position of an individual whale in the next generation of the whale population, and A and C are the coefficient vectors expressed as

$$A = 2 \cdot a \cdot r_1 - a, \tag{22}$$

$$C = 2 \cdot r_2, \tag{23}$$

$$a = 2 - 2 \cdot \frac{t}{T}, \tag{24}$$

where a is the convergence factor, which decreases as the number of iterations increases, and r_1 and r_2 are random numbers between 0 and 1.

3.1.2 Bubble net attack process

This stage is a unique hunting strategy for whales, in which they spiral upward while spitting bubbles, rise to sea surface, and form a net to enclose the prey. The mathematical model of this stage is expressed as

$$W(t+1) = D' \cdot e^{bl} \cdot \cos(2\pi l) + W^*(t), \tag{25}$$

where b is a constant of the logarithmic linear spiral and controls the shape of the logarithmic spiral. It takes the default value of 1. l is a random number between −1 and 1.

To simultaneously update both the encircling predation and air bubble net attack predation, a random parameter p is introduced: if $p < 0.5$, shrinking encircling is performed, and if $p \geq 0.5$, spiral update is performed. These tasks are expressed as

$$W(t+1) = \begin{cases} D' \cdot e^{bl} \cdot \cos(2\pi l) + W^*(t), & \text{if } p \geq 0.5 \\ W^*(t) - A^* D, & \text{if } p < 0.5 \end{cases} \tag{26}$$

where $W(t + 1)$ is the updated position of the next generation of individual whales and p is a random number between 0 and 1.

3.1.3 Random search prey process

In addition to the predation strategies described above, individuals in the whale population also change their position depending on the individuals around them and thus come to search for prey. This action is typical of the exploration phase and is a behavioral mechanism that emphasizes exploration and allows the WOA algorithm to perform a global search. Its mathematical model is given by

$$D = \left| C \cdot W_{rand}(t) - W(t) \right|, \tag{27}$$

$$W(t+1) = W_{rand}(t) - A \cdot D, \tag{28}$$

where W_{rand} represents the individual position of a random whale.

3.2 Improvement strategies

3.2.1 Iteration-based population initialization

In the iterative update of the algorithm, a good or bad position of the initial population directly affects the convergence speed and accuracy of the algorithm. A random initialization of the population can destroy the diversity and convergence of the population. Therefore, the chaos theory in Ref. 16 is introduced to construct the initial population. This strategy produces the initial population by iteration so that the population has better uniformity, randomness, and search space traversal. The mathematical model of this strategy is expressed as

$$W_{i+1} = \sin\left(\frac{r\pi}{W_i}\right), \tag{29}$$

where W_{i+1} is the initial generated population and r is a random number between 0 and 1.

3.2.2 Differential evolution strategy

1. Generate the variant whale population.

This involves randomly selecting the location of any two whales in the current whale population with individuals for information transfer to generate a variant whale location. The specific mathematical model is expressed as

$$V_n(t) = W_n(t) + C * (W_{rand1}(t) - W_{rand2}(t)), \tag{30}$$

where $V_n(t)$ is the individual whale position produced by the variation strategy at the current iteration number, t is the current iteration number, C is the variation operator ranging between 0

and 2, and $W_{rand1}(t)$ and $W_{rand2}(t)$ are the positions of any two whales randomly selected at the current iteration.

2. Generate crossover whale population.

Here, the generated mutant whales and the initial whales are selected and replaced in accordance with the random crossover probability to form a new whale population.

$$U_n(t) = \begin{cases} V_n(t), & \text{if } rand \le CR \\ X_n(t), & \text{if } rand \ge CR \end{cases} \tag{31}$$

$U_n(t)$ is the new whale population generated by the crossover operation at the current iteration, CR is the crossover operator ranging between 0 and 1, and *rand* is a random number between 0 and 1.

3. Select the best whale.

This involves selecting the variant whale individuals and the initial whale individuals in accordance with the magnitude of the fitness function value. The specific mathematical model is given by

$$W_n(t) = \begin{cases} U_n(t), & \text{if } fitness(U_n(t)) < fitness(W_n(t)) \\ X_n(t), & \text{if } fitness(X_n(t)) < fitness(U_n(t)) \end{cases} \tag{32}$$

where $W_n(t)$ is the best whale selected in the current iteration and t is the current number of iterations.

3.2.3 Whale cooperative competition

In the traditional whale algorithm, although each individual in the whale population continuously iterates its position, the whale individuals only rely on the guidance of the following individuals to update their positions. Since there is no information exchange between the whale population individuals, the global solving ability and the solving accuracy of the algorithm cannot be guaranteed. Consequently, a cooperative competition mechanism is introduced to emulate the information transfer process of whales. For each whale $W_i(t)$, another random whale $W_j(t)$ is randomly selected in the population for information exchange. If the fitness function value of the position of whale $W_i(t)$ is better than the fitness function value of random whale $W_j(t)$, then $W_j(t)$ approaches $W_i(t)$ in accordance with Eq. (33) and $W_i(t)$ moves away from $W_j(t)$ in accordance with Eq. (34). Otherwise, the opposite operation is executed. If the whale position is not optimized after the move, this move is cancelled.

$$W_j'(t) = W_j(t) + rand\left(W_i(t) - W_j(t)\right) \tag{33}$$

$$W_i'(t) = W_i(t) + rand\left(W_i(t) - W_j(t)\right) \tag{34}$$

Here, $W_i'(t)$ and $W_j'(t)$ are, respectively, the locations of the *i*th and *j*th individual whales after the cooperative competition mechanism.

3.2.4 Nonlinear fit convergence factor

To accelerate the global survey and local development ability of the algorithm, the convergence factor A is regulated by the strategy of nonlinear fitting to make the algorithm more robust in the updating process:

$$a(t) = -\gamma \cdot \log(t / T), \tag{35}$$

where t is the number of current iterations, T is the maximum number of iterations, and γ is a constant.

3.2.5 Adaptive inertia

To meet the requirements of the whale optimization algorithm to satisfy different stages of the optimization search throughout different iterations and to improve the convergence speed and global convergence, the concept of adaptive inertia weights is introduced into the position update strategy for each whale in the whale population.

$$W(t+1) = \begin{cases} W_{rand}(t) - \omega A \cdot D & |A| > 1 \\ W(t+1) = W*(t) - \omega A \cdot D & \text{if } p < 0.5 \\ W(t+1) = \omega D \cdot e^{bl} \cdot \cos(2\pi l) + W(t) & \text{if } p \geq 0.5 \end{cases} \tag{36}$$

Here, $W(t + 1)$ is the position of the individual whale after the next iteration, $\omega_{\max}$ is the maximum value of the adaptive weights, and $\omega_{\min}$ is the minimum value of the adaptive weights.

As the number of iterations increases, the adaptive weights change. This update mechanism improves the algorithm's local search capacity while increasing its global convergence and speeding up its probability of jumping out of the optimal local solution.

The steps of the IWOADE algorithm are summarized as follows.

Step 1: According to the chaos theory, the iteration-based chaotic initial mapping population of whales is generated using Eq. (29).

Step 2: The following parameters of the optimization algorithm are set: number of populations *Nop*, number of iterations *T*, dimensionality *D*, variation operator *C*, crossover operator *CR*, and bounds of the solution space *up* and *ul*.

Step 3: The mutation operation (crossover strategy) is introduced into the original whale population to generate a new crossover whale population, and the fitness function value of each whale in the crossover population is obtained.

Step 4: The selection mechanism is introduced to replace the whale positions in the corresponding original whale populations with the best whale individuals in the crossover population in order to

form the initial population of new whales using the differential strategy. The individual fitness function values and individual whale positions are then recorded.

Step 5: The whale cooperative competition model is introduced and the positions of whales in the population are updated using Eqs. (33) and (34) to update the individual whale fitness function values and positions.

Step 6: The nonlinear fit convergence factor γ, the variable coefficients A and C, the random probability p, and the adaptive weights w are updated.

Step 7: The whale individual position update mechanism is introduced. More precisely, if $p < 0.5$, when $|A| < 1$, the encircling predation mode is launched. When $|A| \geq 1$, the random search predation mode phase is launched. When $p \geq 0.5$, the whale population selects the spiral strategy to update the population position.

Step 8: It the maximum number of iterations is reached or the output condition is met, step 9 is launched. Otherwise, the update operation in Steps 2–7 is repeated until the condition is met.

Step 9: The current optimal whale individual and the optimal fitness function value are output, and the algorithm ends.

The flowchart of the adaptive swarm nonlinear fitting differential whale algorithm (IOWADE) based on chaos theory is shown in Fig. 3.

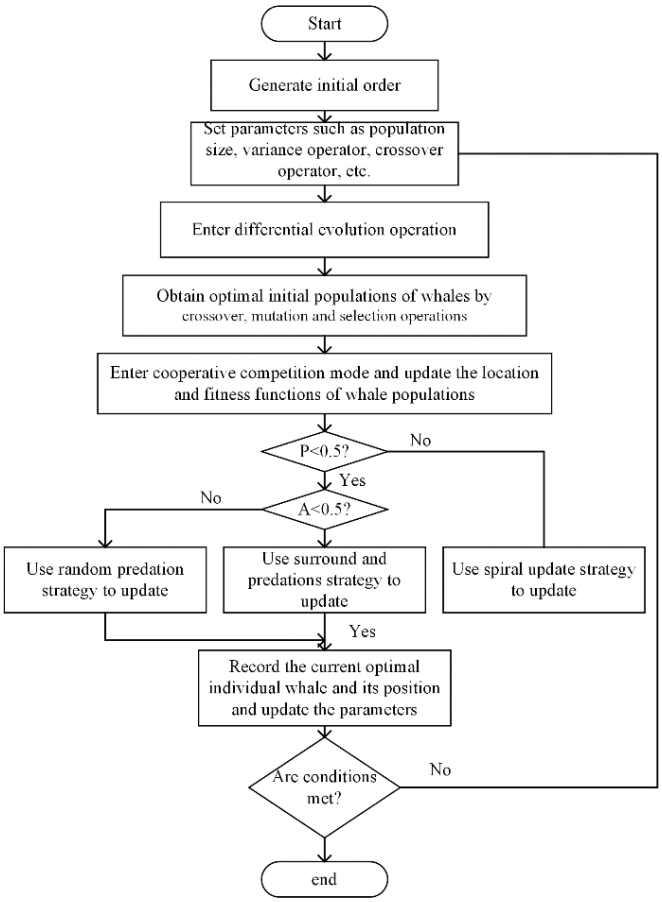

Fig. 3. Flowchart of the adaptive nonlinear fitting differential whale algorithm based on chaos theory.

4. Model Validation and Evaluation

To evaluate the proposed algorithm, a simulation experiment based on an unmanned aircraft logistics scheduling task was conducted. Three rural distribution points and five ground-based cold delivery vehicles were selected as receiving points in one scheduling task. The particle swarm algorithm (PSO), WOA, improved whale optimization algorithm (IWOA),[17] and gray wolf optimization algorithm (GWO) were used in the simulation, and their results were compared.

4.1 Construction of simulation environment

We consider Fengshan County of Guizhou Province as the prototype of the UAV mission environment, as shown in Figs. 4 and 5. The established virtual environment model is shown in Figs. 6 and 7. The towns of Luoqi, Linsang, and Jiangna, respectively numbered 1, 2, and 3, were

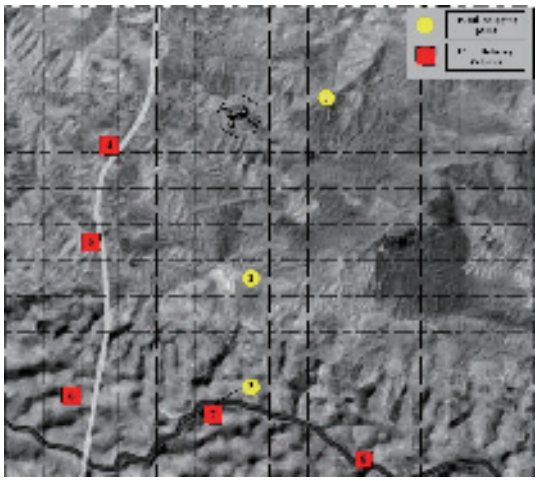

Fig. 4. (Color online) Aerial view of the distribution area

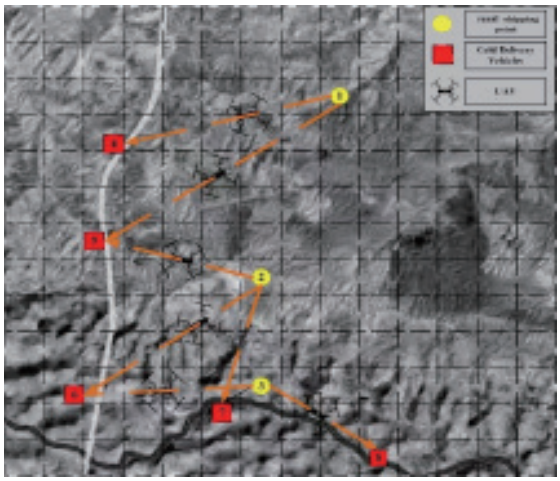

Fig. 5. (Color online) Actual UAV delivery dispatch map.

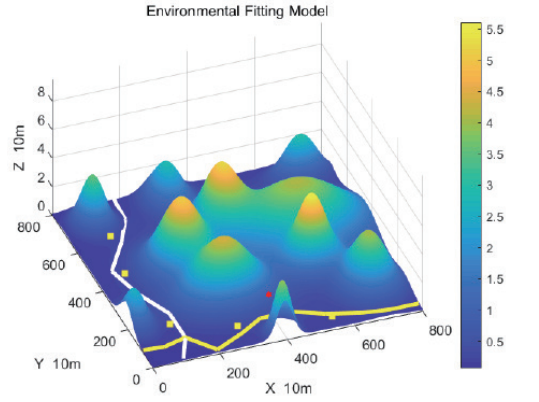

Fig. 6. (Color online) Anthropomorphic mountain model.

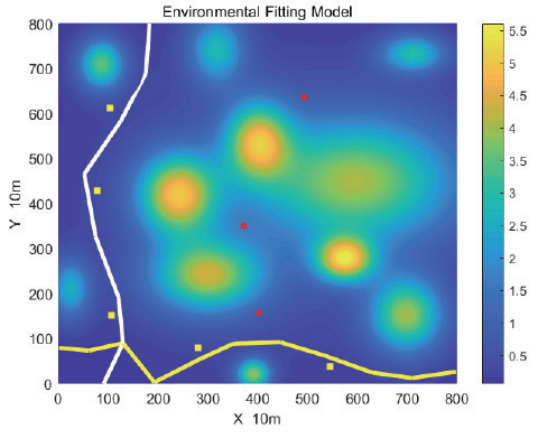

Fig. 7. (Color online) Distribution of shipping and receiving points.

used as the rural shipping points for the UAVs. Wenlin, Panfeng, Xiaotong, Niu Tong, and Iwane were used as receiving stops for the cold delivery vehicle, and are numbered 4, 5, 6, 7, and 8, respectively. Table 2 shows the Manhattan distances between each rural UAV shipping point and cold delivery vehicle stops.

In this study, we use the Mix One multi-rotor UAV as the first-kilometer delivery UAV. According to the information on the official website, the UAV is an oil-electric hybrid UAV. Table 3 shows the performance parameters and data used in the simulation.

4.2 UAV path solution in three-dimensional environment

To obtain delivery routes that satisfy the UAV performance constraints in complex mountainous environments, the IWOADE algorithm is used for UAV path planning; thus, the trajectories of UAVs from each rural distribution point to different cold delivery vehicles are obtained. The planned route maps are shown in Figs. 8–13. Table 4 shows the Euclidean distances between the UAVs at rural shipping points and the cold delivery vehicles.

4.3 UAV mission order allocation

The price of fresh *matsutake* mushrooms is 1500 CNY/kg in July and August, which is the peak season of mushroom growth. The total daily order of *matsutake* mushrooms can reach 1200–1500 pounds. To increase the coordination and controllability of order distribution in the rural areas and improve the economic level of the overall poor mountain farmers, the required orders will be made public, and the three rural areas will jointly fulfill the daily demand of *matsutake* mushroom orders. We use a reasonable UAV dispatch allocation for the *matsutake* orders that each cold delivery vehicle is responsible for in one day. Tables 5 and 6 show the *matsutake* orders of each rugged transport truck and the service time windows of the cold delivery vehicle, respectively.

Table 2
Manhattan distance matrix.

Distance	4 (km)	5 (km)	6 (km)	7 (km)	8 (km)
1	3.9102	4.635	5.963	5.9926	6.1829
2	3.7381	3.042	2.868	3.572	3.2990
3	5.436	4.224	1.445	1.868	2.9404

Table 3
UAV parameters.

Delivery speed (m/s)	15
UAV weight (including battery) (kg)	15.5
UAV cost per kilometer (RMB)	10
Maximum flying altitude (m)	7000
Maximum flight time (min)	300
Maximum range (km)	30
Maximum takeoff weight (kg)	22
Weight of matsutake load (kg)	5

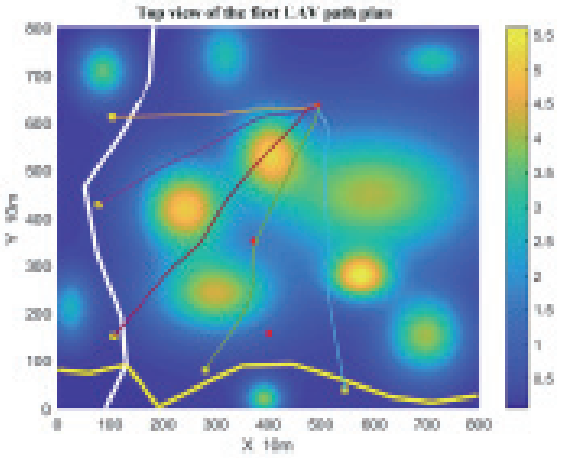

Fig. 8. (Color online) Top view of the first UAV path plan.

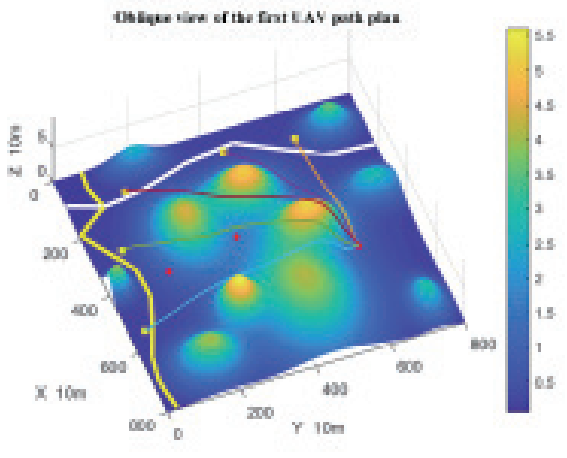

Fig. 9. (Color online) Oblique view of the first UAV path plan.

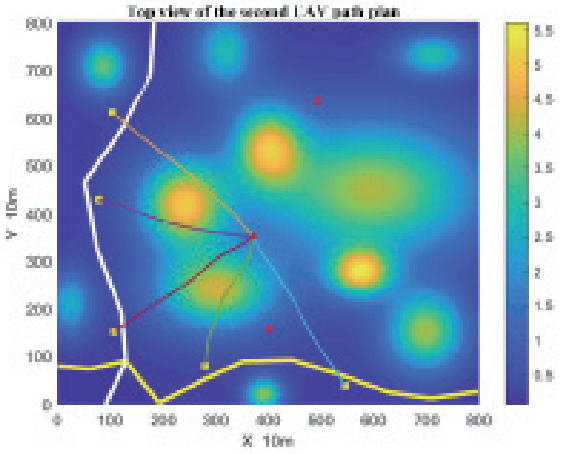

Fig. 10. (Color online) Top view of the second UAV path plan.

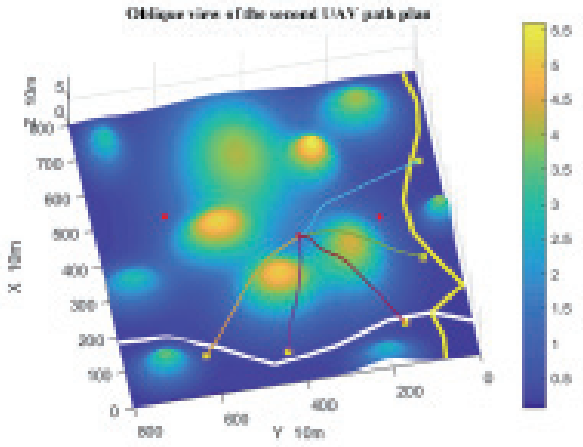

Fig. 11. (Color online) Oblique view of the second UAV path plan.

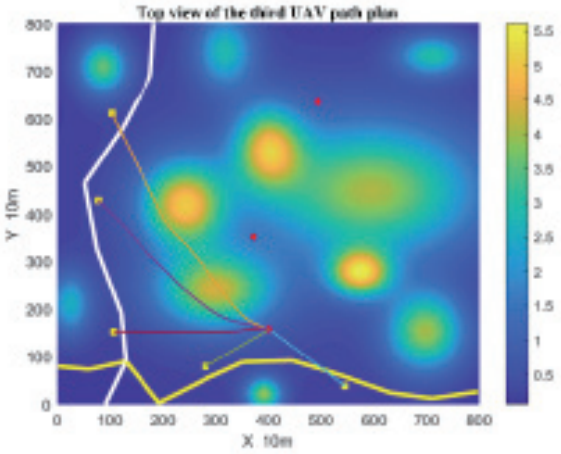

Fig. 12. (Color online) Top view of the third UAV path plan.

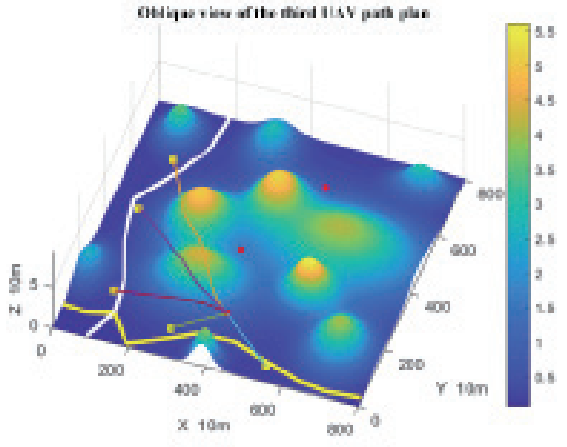

Fig. 13. (Color online) Oblique view of the third UAV path plan.

Table 4
Euclidean distance path.

Distance	4 (km)	5 (km)	6 (km)	7 (km)	8 (km)
1	3.923	4.6951	6.0438	6.039	6.228
2	3.758	3.0623	2.9079	3.5769	3.318
3	5.554	4.3442	1.4451	1.8681	2.9536

Table 5
Matsutake orders (kg).

Weight	4	5	6	7	8
1	483	433	401	487	441

Table 6
Service time windows.

	4	5	6	7	8
Time window	8:10–11:20	9:00–12:00	10:00–1:00	10:30–1:30	11:00–2:00

Table 7
Parameter settings of the proposed algorithms.

Algorithm	Parameter setting	Numerical value
PSO	v_{max}	1
	v_{min}	−1
	c_1	1.5
	c_2	1.5
IWOA	w_{max}	0.9
	w_{min}	0.2
	b	1
DEIWOA	F_0	0.4
	CR	0.1

To determine the optimal scheduling scheme undertaken by each UAV, the PSO, WOA, inertia weight-based whale algorithm (IWOA),[17] gray wolf algorithm (GWO), and proposed DEIWOA are used to solve the model. The settings of the proposed algorithms were selected to ensure the fairness of the comparison and are shown in Table 7.

Figure 14 shows the evolutionary curve of the fitness function for each algorithm run once. Figure 15 shows the evolutionary curve of the fitness function averaged over thirty runs of each algorithm. Table 8 shows the data obtained by the algorithms. Table 9 shows the best UAV order scheduling scheme planned by the proposed algorithms.

From Figs. 14 and 15 and Table 8, it can be seen that PSO, WOA, IWOA, GWO, and the proposed DEIWOA all have a strong search capability and global convergence. From Table 8, the proposed optimization algorithm is seen to show an improvement of 39, 50, 36, and 23% in solving the logistics order scheduling problem, compared with PSO, GWO, WOA, and IWOA, respectively.

Because of the randomness of the population intelligence optimization algorithm in solving large-scale problems, to ensure the accuracy of the experiment, the adaptation function of each algorithm used to solve the same logistics scheduling order problem was applied 30 times. The results of simulation experiments show that our proposed DEIOWA algorithm exhibits excellent stability as well as searchability after thirty runs. Figure 16 shows the metrics embodied by each

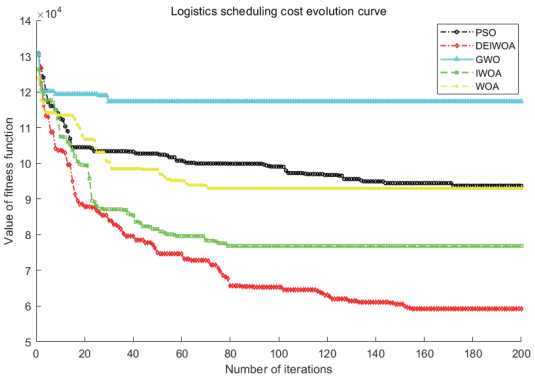

Fig. 14. (Color online) Evolutionary curve of the fitness function for each algorithm run once.

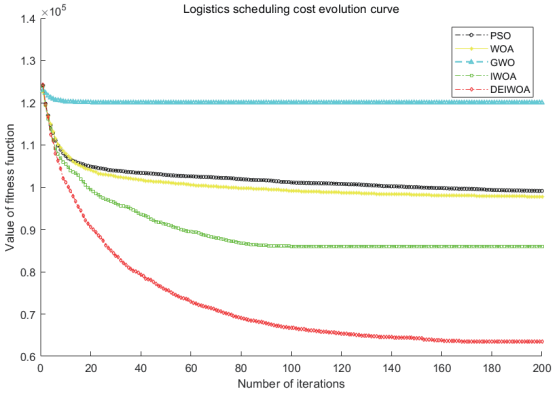

Fig. 15. (Color online) Evolutionary curve of the fitness function averaged over thirty runs of each algorithm.

Table 8
Simulation data.

Indicators	Algorithm				
	PSO	WOA	IWOA	GWO	DEIWOA
Fitness	9.372×10^4	9.3×10^4	7.68×10^4	1.173×10^4	5.918×10^4
Average fitness	9.914×10^4	9.774×10^4	8.603×10^4	1.2×10^4	6.342×10^4

Table 9
UAV logistics dispatch distribution solution.

UAV number	UAV delivery order sequence
1	56→84→111→139→167→170→195→227
2	12→41→69→98→133→162→190→219
3	39→42→70→105→134→163→191→220
4	22→43→71→104→136→166→194→225
5	47→79→82→112→140→168→196
6	48→53→75→110→137→164→192→221
7	49→72→86→99→131→159→189→217
8	2→44→73→100→135→165→193→222
9	31→49→59→87→114→145→171→199
10	31→32→64→94→122→155→182→210
11	5→33→60→92→120→150→177→207
12	3→34→61→88→115→148→174→201
13	35→48→65→95→126→156→184→214
14	26→36→66→89→119→152→175→205
15	6→37→58→91→118→149→176→206
16	38→46→67→90→125→154→181→209
17	39→62→86→113→144→173→200
18	33→40→68→93→121→151→178→208
19	13→50→80→101→128→157→186→213
20	24→51→76→96→116→141→179→211
21	7→52→77→97→117→142→169→197→223
22	29→63→102→104→123→146→180→212
23	45→55→74→106→138→161→188→216
24	18→53→81→108→130→160→187→215
25	30→57→85→127→147→172→185→198→218
26	46→78→91→107→129→153→183→203→228
27	42→54→82→109→132→158→185→204→226
28	35→55→83→103→124→143→170→202→224

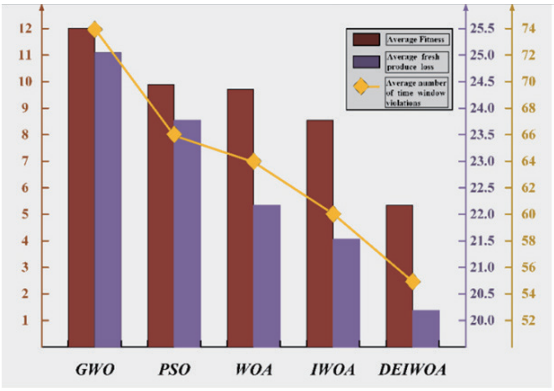

Fig. 16. (Color online) Simulation results analysis picture.

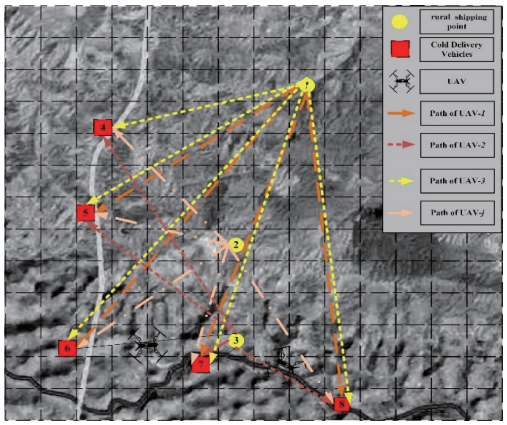

Fig. 17. (Color online) Actual UAV logistics dispatching distribution scheme.

algorithm. The proposed DEIWOA reduces the consumption cost of solving the scheduling problem by 35720, 56580, 34320, and 22610 CNY and increases the economic return by 36, 47, 35, and 26% compared with the PSO, WOA, IWOA, and GWO, respectively. Finally, Fig. 16 shows the raw loss cost of fresh produce and the average number of time window violations during the drone delivery process using DEIWOA as 2025.6CNY and 55 violations, respectively. Compared with the PSO, WOA, IOWA, and GWO algorithms, our proposed DEIOWA algorithm can also effectively reduce the raw loss cost while enabling the UAV to reach the cold delivery vehicle on the ground within the specified time. Figure 17 is a schematic diagram of some UAV mission delivery. The obtained results show that the introduction of chaotic mapping of the initial population, the DE strategy, the cooperative competition mechanism, the nonlinear fitting convergence factor, and inertia weights significantly improves the global search capability, robustness, and convergence of the whale algorithm, effectively avoiding the problem of traditional algorithms falling into local optima when solving large-scale complex problems.

Therefore, the proposed DEIWOA algorithm is more efficient in solving the UAV logistics scheduling problem than the PSO, WOA, IWOA, and GWO algorithms. It can also better handle such complex and large-scale problems.

5. Conclusion

To solve the problem of “first kilometer” delivery in rural mountainous areas, in this paper, we proposed a delivery method using UAVs as a carrier. Several constraints, such as UAV performance, delivery time window, new loss cost, and UAV delivery cost, were considered, and a multi-UAV logistics delivery model was proposed. An adaptive nonlinear fitting whale algorithm based on chaos theory was proposed to solve the model and deal with the problem faced by the traditional whale optimization algorithm, which has poor global searchability and quickly falls into a local optimum. In solving the UAV delivery path, the static path of the UAV was first solved using the IWOADE algorithm. In the actual UAV delivery process, multisource heterogeneous

sensors are loaded onto the UAV to help the UAV achieve dynamic obstacle avoidance in the actual flight process. Finally, the logistics distribution model was solved using the IWOADE algorithm to obtain the optimal UAV delivery scheme. Comparison with the PSO, WOA, IWOA, and GWO algorithms showed that the proposed IWOADE algorithm outperforms these algorithms in terms of solution accuracy, global convergence, and robustness, which further verifies the superiority and adaptability of IWOADE.

Acknowledgments

This work was supported in part by the Science and Technology Project of China Southern Power Grid Co., Ltd. under Grants YNKJXM20220174, YNKJXM20220010.

References

1 Y. Wang, J. Zhang, and Y. Liu: Control and Decis. **35** (2020) 1606 (in Chinese). https://doi.org/10.13195/j.kzyjc.2018.1662
2 X. Ren, H. Huang. Yu, and Y. Shao: Control and Decis. **36** (2021) 2313 (in Chinese). https://doi.org/10.13195/j.kzyjc.2020.1315
3 K. Dorling, J. Heinrichs, G. G. Messier, and S. Magierowski: IEEE Trans. Syst. Man Cybern. Part A Syst. **47** (2017) 70. https://doi.org/10.1109/TSMC.2016.2582745
4 C. Yaoting and H. Heliang: China Bus. Market **31** (2021) 10 (in Chinese). https://doi.org/10.14089/j.cnki.cn11-3664/f.2017.02.002
5 Z. Honghai, L. Han, and L. Mou: J. Transp. Syst. Eng. Inf. Technol. **20** (2020) 22 (in Chinese). https://doi.org/10.16097/j.cnki.1009-6744.2020.06.003
6 Z. Qiqian, X. Weiwei, and Z. Honghai: J. Beijing University of Aeronautics and Astronautics **46** (2020) 1275 (in Chinese). https://doi.org/10.13700/j.bh.1001-5965.2019.0455
7 S. I. Khan, Z. Qadir, H. S. Munawar, S. R. Nayak, A. K. Budati, K. D. Verma, and D. Prakash: Phys. Commun. **47** (2021) 101337. https://doi.org/10.1016/j.phycom.2021.101337
8 F. Causa and G. Fasano: Aerosp. Sci. Technol. **110** (2021) 106507. https://doi.org/10.1016/j.ast.2021.106507
9 W. C. Chiang, Y. Li, J. Shang, and T L. Urban: Appl. Energy **242** (219) 1164. https://doi.org/10.1016/j.apenergy.2019.03.117.
10 Y. N. Yin, X. J. Wu, and C. Y. Zhang: J. Hebei University of Science and Technology **42** (2021) 38 (in Chinese). https://doi.org/10.7535/hbkd.2019yx06010
11 Z. Li, W. X. Li, and Y. X. Ju: J. Wuhan University of Technology (Transportation Science & Engineering) **43** (2019) 761 (in Chinese). https://doi.org/10.3963/j.issn.2095-3844.2019.04.036
12 J. Zheng: IEEE Access **8** (2020) 39439. https://doi.org/10.1109/ACCESS.2020.2974774
13 H. M. Fan. W. Q. Liu, and Z. L. Xu: Comput. Eng. Appl. **54** (2018) 221 (in Chinese). https://doi.org/10.3778/j.issn.1002-8331.1803-0155
14 Y. Lu, J. Gu, D. Xie, and Y. Li: IEEE Access **7** (2019) 122238. https://doi.org/10.1109/ACCESS.2019.2937910
15 R. Tiwari, G. Jain, and A. Shukla: Int. J. Comput. Sci. Eng. Int. **37** (2019) 101016. https://doi.org/10.1016/j.jocs.2019.07.003
16 Y. Liu, Y. Yuan, H. Guan, X. Sun, and C. Huang: Res. Transp. Bus. Manage. **37** (2021) 101016. https://doi.org/10.1016/j.rtbm.2020.100487
17 S. Q. Wu and Z. Y. Cai: Mech. Electr. Eng. Technol. **48** (2019) 83 (in Chinese). https://doi.org/10.3969/j.issn.1009-9492.2019.10.027